博士学位論文

Intracellular traffic pathway of STING upon its ligand stimulation

(DNA ウイルスセンサーSTING の細胞内輸送経路の解明)

向井 康治朗

Kojiro Mukai

Contents

Introduction

The innate immune system has evolved to protect host cells from various invading pathogens. These innate immune responses are triggered by the recognition of pathogen components with germline-encoded pattern-recognition receptors (PRRs) including NOD-like receptors (NLRs; also known as nucleotide-binding domain and leucine-rich repeat containing molecules), cytosolic RIG-I-like receptors (RLRs), and membrane-bound Toll-like receptors (TLRs) (*1-4*). The recognition initiates signal transduction pathways leading to the induction of type I interferons (IFNs) and proinflammatory cytokines, which are essential for innate and subsequent adaptive immune responses (*5*).

Previous studies showed that DNA derived from DNA viruses, bacteria and even from host cells is often act as PAMPs and consequently triggers the innate immune responses (*6*). For example, it is well known that extracellular CpG DNA is recognized by TLR9 and facilitates the induction of the cytokines including Type I IFNs (*7, 8*). In addition, STimulator of INterferon Genes (STING; also known as MITA, ERIS, MPYS, TMEM173) was recently discovered as essential protein for response to aberrant cytosolic DNA species and for the production of host defense genes such as type I IFNs (*9-12*). STING-deficient cells display profound defects in producing IFNβ and other proinflammatory cytokines upon infection of DNA virus such as herpes simplex virus 1

(HSV-1) or of Listeria monocytogenes (*13*). Moreover, STING$^{-/-}$ mice are more susceptible to lethal infection after exposure to HSV-1 (*13*).

STING is an endoplasmic reticulum (ER)-resident transmembrane protein, which binds to dsDNA (*14*) and cyclic di-nucleotides (CDNs) including cyclic di-GMP-AMP (cGAMP) generated from certain intracellular bacteria or via a DNA-binding host protein cGAS (cGAMP synthase; also known as MB21D1 or C6orf150) (*15-19*). Upon DNA virus infection, cGAS is activated by cytosolic virus dsDNA and catalyzes the synthesis of cGAMP from ATP and GTP. After binding to cGAMP, STING activates protein kinase TBK1, which in turn phosphorylates transcription factor IRF3 directly and also activates NF-κB pathway (*13, 20, 21*). Then, phosphorylated IRF3 and activated NF-κB translocate to the nucleus to initiate the transcription of numerous innate immune genes, including type I IFNs and proinflammatory cytokines.

Interestingly, STING rapidly translocates from the ER to perinuclear compartments including the Golgi, endosomes, and autophagosome-like structures upon DNA virus, dsDNA and cGAMP stimulation (*13, 15, 22*). Although previous studies showed that only cytosolic factors consisting of CDNs, the cytosolic region of STING, and TBK1 are sufficient to activate IRF3 in vitro (*20, 23, 24*), this translocation of STING from the ER suggests other cellular factors to regulate the activation of STING.

Here I first show the precise translocation pathway of STING upon its stimulation. STING sequentially translocates from the ER through the Golgi, recycling endosomes (REs), and p62-positive punctate structures, then eventually to lysosomes where STING is degraded. I found that TBK1 activation occurs at the Golgi, more specifically, at the

trans-Golgi network. I further found that STING is subjected to palmitoylation at the Golgi and that this palmitoylation is required for its activation. Therefore, this study uncovers the novel post-translational modification that is essential for STING activation and would shed light on the development of drugs for autoimmune diseases.

Results

Translocation of STING from the ER upon its stimulation

Previous studies have shown that STING translocates from the ER to perinuclear compartments that include the Golgi and endosomes, upon the stimulation with the transfected dsDNA, cGAMP, or the infection with DNA-viruses (*13, 15, 22*). But, how this translocation relates to the activation of downstream of STING, such as phosphorylation of TBK1 and IRF3, is not known. To examine the relationship of intracellular translocation of STING and the timing of its activation, I decided to perform the experiments in COS-1 cells, which are a cell line with distinctly separate organelles, therefore are suitable for the precise localization of Golgi/endosomal proteins (*25*). COS-1 cells were retrovirally transfected with EGFP-mouse STING (EGFP-mSTING) and selected for its stable expression. I used this cell line (emsCOS-1 cells: EGFP-mouse STING-COS-1 cells) throughout the present experiments. Among several STING activators, I chose a cell-permeable low-molecular compound DMXAA that is specific for mouse STING. Because emsCOS-1 cells express mSTING, DMXAA could activate all the cells, making the following biochemical experiments feasible. On the other hand, the transfection of dsDNA activates at most 10 - 20% cells because of its transfection efficiency.

The mRNA of IFNβ, TNF-α, IL-6, and IL-8 are known to be induced by STING activation with DMXAA (*13, 14*). As shown in Fig. 1, those mRNAs were significantly induced in emsCOS-1 cells 8 - 12 hours after by DMXAA treatment, showing that the

cells respond properly to the STING activation.

The subcellular localization of EGFP-mSTING was next examined. Without DMXAA stimulation, STING co-localized with an ER marker (calreticulin) (Fig. 2A), being consistent with the ER localization of STING in unstimulated cells as previously described (*9, 13, 14*). After a 20-120-min stimulation, STING co-localized with GM130 (Fig. 2A). After a 240-min stimulation, STING concentrates within the Golgi circle (Fig. 2A), and co-localized with a REs marker Rab11 (Fig. 3A). After a 480-min stimulation, STING co-localized with p62, a ubiquitin-binding autophagic adaptor protein (Fig. 3A). These results indicated that STING translocates from the ER through the Golgi and REs, then to the p62-positive punctate structures.

STING was gradually degraded after a 480-min stimulation, and further degraded after a 720-min stimulation (Fig. 3B). This decrease was completely abolished by chloroquine, a lysosomal inhibitor, but not by a proteasomal inhibitor MG132 (Fig. 3B). In the presence of chloroquine, a portion of STING appeared very close to, or within lysosomal compartments after a 720-min stimulation (Fig. 3C). These results suggested that STING translocates to lysosomes after its exit from p62-positive compartments and is degraded in lysosomes.

In summary, I found that STING translocates sequentially from the ER, through the Golgi, REs, p62-positive compartments, then finally to lysosomes after its stimulation.

Translocation of STING to the Golgi is required for activation of TBK1

The phosphorylation of TBK1 and IRF3 occurs by STING-dependent fashion (*10,*

15, 21). I found that DMXAA treatment induced phosphorylation of TBK1 after a 60-min stimulation and that of IRF3 between 60 and 180 min after stimulation (Fig. 4). In the previous section, I found that STING localized exclusively at the Golgi during that timing (60 to 180 min after stimulation), suggesting that STING activates TBK1 and IRF3 at the Golgi, not at the ER.

To examine if the transport of STING to the Golgi is required for the activation of TBK1, *i.e.*, the phosphorylation of TBK1, I sought to block the STING traffic to the Golgi. For this purpose, I used brefeldin A (BFA) that inhibits the traffic from the ER (*26, 27*). emsCOS-1 cells were pretreated with BFA for 30 min and then stimulated with DMXAA. The transport of STING from the ER to the Golgi was impaired in the presence of BFA, even up to 480 min after DMXAA stimulation (Fig. 5A). Under this condition, the phosphorylation of TBK1 was completely abolished (Fig. 6). These results suggest that the transport of STING to the Golgi is required for the activation of TBK1.

Next I examined the effect of the block of STING transport from the Golgi. emsCOS-1 cells were pretreated at 20^{o}C, in which the traffic from the Golgi is impaired (*28*), then simulated with DMXAA. As shown in Fig. 5B, STING reached the Golgi 60 min after stimulation and still localized at the Golgi even 480 min after stimulation. These results showed that STING cannot exit the Golgi at 20^{o}C. Under this condition, the phosphorylation of TBK1 was detected at the similar extent to the control condition at 37^{o}C (Fig. 6). The slight delay of the timing of TBK phosphorylation may be due to the delay of the traffic of STING. These results emphasize that the Golgi is the

intracellular site where STING activates TBK1.

TBK1 is activated at the trans-Golgi network

Ser-172 of TBK1 is autophosphorylated in its activation loop, and autophosphorylation is essential for triggering TBK1-dependent signaling (*29*). To further characterize the intracellular site where TBK1 is activated by STING, I examined the subcellular localization of p-TBK1 (Ser-172) by immunocytochemistry. The fluorescence of p-TBK1 was not detected after a 20 min-stimulation, but detected after a 60-min stimulation (Fig. 7), being consistent with the biochemical data (Fig. 4). These results raised an interesting possibility that STING may activate TBK1 at a specific subcompartment of the Golgi, since STING started to localize at the Golgi after a 20 min-stimulation with no obvious TBK1 activation (Fig. 4 and 7). Therefore, I sought to determine the precise localization of p-TBK1 within the Golgi.

For this purpose, I used nocodazole that inhibits polymerization of microtubules (*30*). The treatment of cells with nocodazole is known to disperse the Golgi into the cytoplasm, generating "mini-Golgi" in which the polarity of the Golgi, *i.e.*, *cis* to *trans*, is visually separated under the fluorescence microscope (*31*). As shown in Fig. 8B, STING was dispersed into the cytoplasm in cells treated with DMXAA and nocodazole. One STING-positive puncta (indicated by arrowhead in Fig. 8B) was magnified in Fig. 8C. In this puncta, cis-Golgi positive with GM130 (cyan) was located at the upper-left and trans-Golgi network (TGN) positive with TGN46 (magenta) was located at the bottom-right. STING (green) distributed at both sides of the Golgi, however, p-TBK1

was exclusively localized within the TGN, not at cis-Golgi. The fluorescence intensity profile along white arrow supported this observation (Fig. 8D). Other STING-positive puncta consistently showed that p-TBK1 was associated with TGN, but not with cis-Golgi (data not shown). These results suggested that TBK is activated at the TGN.

STING becomes palmitoylated at the Golgi

As shown above, the translocation of STING from the ER to the Golgi is required for TBK1 activation, and the activated form of TBK1, *i.e.*, p-TBK1, is specifically localized in the TGN. I reasoned that some biochemical modification(s) of STING may allow the specific activation of STING at the TGN. Previous study showed that STING can be phosphorylated (*10, 15, 20*) or ubiquitinated (*5, 32-35*) (cartooned in Fig. 9A), therefore I first examined if these modifications explain the activation of STING at the TGN.

Phosphorylation of STING was validated by phos-tag SDS-PAGE. Before and after the stimulation with DMXAA (30 - 120 min), the mobility of STING in phos-tag gel did not change (Fig. 9B), indicating that STING did not receive simulation-dependent phosphorylation. Ubiquitination of STING was validated in cells that were transfected with Myc-tagged ubiquitin. After a 60-min simulation with DMXAA, the cell lysate was Immunoprecipitated with anti-GFP antibody and then blotted with anti-GFP. As shown in Fig. 9C (the middle panel), there was no obvious difference of the abundance and the molecular weight of STING before and after the stimulation. The immunoprecipitates were also blotted with anti-Myc for the presence

of ubiquitin (Fig. 9C, the right panel). I did not detect any clear signal of ubiquitin before and after the stimulation. These results indicate that STING did not receive ubiquitination under this experimental condition.

The contribution of phosphorylation and ubiquitination of STING for its activation was also validated using COS-1 cells that stably express mutant STING that are resistant to these modifications (S357A, S365A, or K150R/K151R). As shown in Fig. 10A and B, all these mutant still induced the phosphorylation of TBK1 after the DMXAA stimulation within 60 min. Therefore, at least under this experimental condition, phosphorylation and ubiquitination may not be essential the STING activation at the Golgi.

Recent studies reveal that the Golgi serves as palmitoylation machinery (*36, 37*). I wonder if the palmitoylation of STING may be required for the STING activation. To examine if the palmitoylation is involved in such process, emsCOS-1 cells were treated with 2-bromopalmitate (2-BP), a palmitoylation inhibitor, prior to the DMXAA stimulation. As shown in Fig. 11A, 2-BP significantly suppressed the induction of IFNβ, TNFα, IL-6, and IL8. 2-BP also suppressed the phosphorylation of TBK1 (Fig. 11B). These results suggested that palmitoylation is involved in the activation of TBK1. The translocation of STING from the ER to the Golgi is not prevented with 2-BP treatment (Fig. 12).

To examine whether STING is palmitoylated, I took a metabolic labelling approach. emsCOS-1 cells were incubated with [^{3}H] palmitate and then stimulated with DMXAA. As shown in Fig. 13A, STING incorporated label from [^{3}H] palmitate after

the stimulation and this signal was completely abolished when 2-BP was included (Fig. 13B). These results suggested the stimulation-dependent palmitoylation of STING. It is of note that the significant incorporation of [^{3}H] to STING was observed after a 60-min stimulation, in which STING started to localize to the TGN.

Palmitoylation of STING is required for activation of TBK1

Protein palmitoylation occurs on Cys residues. STING has eight Cys residues (Cys64, Cys88, Cys91, Cys147, Cys205, Cys256, Cys291, and Cys308), which are conserved among several mammalian species (Fig. 14). Besides the eight Cys residues, mouse STING has additional Cys65. To elucidate the site(s) of palmitoylation of STING, COS-1 cells that stably express STING with "Cys to Ser" mutation (C64S/C65S, C88S/C91S, C147S, C205S, C256S, C291S, or C308S) were established. The palmitoylation of these mutants was examined by metabolic labelling with [^{3}H] palmitate. As shown in Fig. 15, the incorporation of [^{3}H] from palmitate into STING was significantly reduced in C88S/C91S mutant. The other STING mutants showed fewer or no reduction (data not shown), indicating that Cys88 and/or Cys91 are the primal Cys residues that become palmitoylated upon DMXAA stimulation. C88S/C91S could not induce the transcription of IFNβ, TNFα, and IL-8 (Fig. 16). C88S/C91S translocated from the ER to the Golgi upon DMXAA stimulation as WT STING (Fig. 17), suggesting that the mutations did not affect the binding of DMXAA. Together, these results suggested that the stimulation-dependent palmitoylation of Cys88 and/or Cys91 renders STING to activate IRF3 and NF-κB pathway.

Discussion

In the present study, I elucidated the exact intracellular trafficking pathway of STING, a critical cytosolic ds-DNA sensor. STING exits the ER to the Golgi within 10 min after DMXAA stimulation, and stays in the Golgi for 2 hours. STING further moves to the REs (2 - 4 hours), to the p62-positive structures (4 – 12 hours), then to lysosomes where STING is degraded. During the stay in the Golgi, more specifically at the TGN, STING activates TBK1 that is a downstream kinase of STING and required for the interferon responses. Previous studies suggested that STING ligands, such as cyclic dinucleotides (CDNs) or DMXAA, alter the conformation of STING, allowing STING to activate TBK1 directly (*20, 23, 24*). In contrast, the present study suggests that STING ligands function as an inducer of STING translocation from the ER. How the stable association of STING with the ER is disrupted after the ligand binding remains to be elucidated.

I found that STING is subjected to palmitoylation at the Golgi and further provide evidence that the palmitoylation is the critical factor for STING activation. Palmitoylation occurs on cysteines 88 and/or 91 of STING and mutations of these cysteines mostly abolished the ability of STING to activate TBK1. The palmitoylation provides another membrane anchoring site of cytoplasmic region of STING. This may result in the conformational change of the cytoplasmic region that allows the exposure of latent TBK1 binding site or may increase the affinity of STING with “raft lipid” (*38*), through which STING would cluster to facilitate TBK activation.

Recent studies suggested that autophagy-related proteins, such as ATG9 and ULK1, contribute to the degradation of STING (*15*). ULK1 that is a serine/threonine-protein kinase and localizes at REs (*39*), directly phosphorylates STING (*15*). Together with the present findings that STING translocates from the ER through the Golgi and REs to lysosomes, ULK1 may function in the correct sorting of STING to lysosomes through the phosphorylation of STING at REs. In addition to phosphorylation, STING is known to be subjected to ubiquitination (*5, 32-35*). I did not detect significant ubiquitination of STING at the Golgi and therefore the ubiquitination appears not essential for the activation of STING. However, it remains possible that ubiquitination is required for the post-Golgi traffic of STING to lysosomes.

Previous studies indicated that STING can translocate to mitochondria-associated membrane (MAM) upon the infection of RNA viruses (*10, 32*), and facilitates the induction of interferon responses. It would be interesting to examine if the activation of STING at MAM needs palmitoylation, as is the case of STING activation at the Golgi. It would be also interesting to examine the fate of activated STING at MAM. emsCOS-1 cells that I established in this study should be useful for this purpose.

A gain-of-function mutation (V155M) in STING is recently found in patients that exhibit a complex systemic inflammatory syndrome associated with pulmonary fibrosis and autoimmunity (*40, 41*). Quite interestingly, STING (V155M) localizes in the Golgi in the patient fibroblasts and is constitutively active (*41*), which correlate with the findings of the present study that shows that the Golgi is the intracellular site for the activation of STING. It would be worth examining if STING (V155M) needs

palmitoylation for its activity. If the inhibition of palmitoylation suppresses the activity of STING (V155M), palmitoylation inhibitor may hold promise for treating such patients.

Recent studies show that STING plays important roles in the elimination of cancerous cells (*42, 43*) and the process of apoptosis (*44, 45*), besides in the defense against viruses. Understanding the molecular mechanism underlying the activation of STING, such as identification of palmitoylation enzymes at the Golgi, should shed light on the development of drugs for autoimmune diseases and cancer.

Material & Methods

Antibodies. The following antibodies were purchased from the manufacturers as noted: mouse anti-GFP (JL-8, Clontech); mouse anti-GFP (3E6, Invitrogen); rabbit anti-TBK1 (abcam); rabbit anti-phosphoTBK1 (Cell Signaling); rabbit anti-IRF3 (Santa Cruz); rabbit anti-phosphoIRF3 (Cell Signaling); rabbit anti-Rab11 (Zymed); mouse anti-p62 (BD Transduction Laboratories); anti sheep anti-TGN46 (Serotec); mouse anti-Calreticulin (BD Biosciences); mouse anti-LAMP1 (H4A3; BD Biosciences); mouse anti-α-tubulin (DM1A; SIGMA); mouse anti-myc (9E10; Sigma); mouse anti-GM130 (BD Biosciences); and Alexa 488-, 594-, or 647-conjugated secondary antibodies (Invitrogen); sheep anti-mouse IgG antibody-HRP, donkey anti-rabbit IgG antibody-HRP (GE Healthcare).

Reagents

The following reagents were purchased from the manufacturers as noted: DMXAA (Sigma), 2-Bromopalmitic acid (Wako), Palmitic acid [9,10-^{3}H(N)] (American Radiolabeled Chemicals, Inc.), Brefeldin A (SIGMA), Nocodazole (SIGMA).

Plasmids

The following genes were amplified by polymerase chain reaction (PCR) with cDNA derived from mouse (ICR) liver using the following primers: 5'-CCCGAATTCAATGCCATACTCCAACCTGCA-3' (mSTING; sense primer, EcoRI

site is underlined) and 5'- CCCGCGGCCGCTCAGATGAGGTCAGTGCGGA-3' (mSTING; antisense primer, NotI site is underlined). The products encoding mSTING was introduced into pMXs-IP-GFP, to generate N-terminal GFP-tagged constructs.

Cell culture and transfection

COS-1 cells stably expressing EGFP-mSTING were generated as follows: HEK293T cells were transiently transfected using Lipofectamine 2000 (Invitrogen) reagent with pMXs-IP-EGFP-mSTING together with pCG-VSV-G and pCG-gag-pol to render retroviruses infectious to human cells. The retroviruses were added to COS-1 cells and selected with puromycin. Cells were cultured in DMEM supplemented with 10% fetal bovine serum (FBS) and Penicillin-Streptomycin-Glutamine (PSG) in a 5% CO2 incubator.

Immunocytochemistry

Immunocytochemistry was performed as described previously (Uchida et al., 2011). When I evaluated the traffic, cyclohexamide (1 μg/mL) was added to the cells to inhibit the newly synthesized STING. Briefly, cells were fixed with pre-warmed 4% paraformaldehyde in PBS at room temperature for 15 min, permeabilized with 0.1% Triton X-100 in PBS at room temperature for 5 min, and quenched with 50 mM NH4Cl in PBS at room temperature for 10 min. After blocking with 3% BSA in PBS, cells were incubated with 1st antibodies. For LAMP1 staining, fixed cells were permeabilized with 0.1% saponin in PBS for 10 min at room temperature before blocking.

Confocal microscopy

Confocal microscopy was performed using a TCS SP8 (Leica) with a 63 x 1.2 Plan-Apochromat water immersion lens.

Western blotting

COS-1 cells stably expressing EGFP-mSTING were stimulated with DMXAA in growth medium. After stimulation, cells were washed with PBS, and scraped in 1 x Laemmli sample Buffer without BPB and DTT. After the protein concentrations of samples were determined by the bicinchoninic acid (BCA) assay (Pierce), BPB (final 0.001%) and DTT (final 100 mM) were added to the lysate. Then the lysate were boiled at 95C for 10 min. Proteins were separated by 10% polyacrylamide gel and then transferred to polyvinylidene difluoride membranes (Millipore). The membranes were blocked for 1 h using 10 mM Tris-HCl (pH 7.4)/150 mM NaCl/0.05% Tween-20/5% skim milk. The membranes were incubated with primary antibodies, followed by secondary antibodies conjugated to peroxidase. The proteins were visualized by chemiluminescence using ImageQuant LAS4000 (GE Healthcare).

For phos-tag western blotting, proteins were separated by 6% polyacrylamide gel containing 100 μM phos-tag at 4 °C for overnight (2 mA, C.C.), according to the manufacturer's instructions.

Immunoprecipitation

Cells were washed with ice-cold PBS, and scraped in immunoprecipitation buffer

composed of 50 mM HEPES-NaOH (pH 7.2), 150 mM NaCl, 5 mM EDTA, 1% Triton X-100, 1 mM PMSF, protease inhibitors (10 μg/mL Leupeptin, 10 μg/mL Pepstatin, 10 μg/mL Aprotinin), phosphatase inhibitors (8 mM NaF, 12 mM beta-glycerophosphate, 1 mM Na_3VO_4, 1.2 mM Na_2NoO_4, 5 μM Cantharidin, 2 mM Imidazole), 10 mM NEM. The cell lysates were centrifuged at 15,000 g for 10 min at 4 °C, and the resultant supernatants were pre-cleared with protein G sepharose fast flow (GE Healthcare) at 4°C for 30 min. Then after BCA assay, the lysates were diluted to the same concentration with immunoprecipitation buffer. The lysates were incubated for overnight at 4°C with anti-GFP (3E6). The beads were washed four times with immunoprecipitation wash buffer (50 mM HEPES-NaOH (pH7.2), 150 mM NaCl, 0.1% Triton X-100). Immunoprecipitated proteins were analyzed by western blotting.

Metabolic labelling with [3H]-palmitate and immunoprecipitation

Cells were incubated in DMEM containing 0.1% essentially fatty acid free BSA and PSG for 60 min at 37 °C before incubation with 0.1 mCi/ml [^{3}H] palmitic acid for 1 h at 37 °C. Then DMEM containing DMXAA (final 25 μg/mL) was added to the cells. After DMXAA stimulation, cells were washed with ice-cold PBS, scraped in immunoprecipitation buffer without detergent. After centrifugation at 1000 rpm for 3 min at 4 °C, the pellets were lysed with immunoprecipitation buffer with 1% SDS, mixed with vortex, and sonicated on ice. Then the lysates were diluted by 0.1% SDS with immunoprecipitation buffer. After centrifugation at 15000 rpm for 10 min at 4 °C and BCA assay, and the lysates were diluted to the same concentration with

immunoprecipitation buffer. Then the immunoprecipitation was performed as described above.

Total RNA Isolation and Quantitative Real-time PCR

Total RNA from cells was extracted using Isogen II (Nippongene, Toyama, Japan), purified using High Pure RNA Tissue kit (Roche), and reverse-transcribed using the High Capacity cDNA Reverse Transcription kit (Applied Biosystems, Foster City, CA). Quantitative real-time PCR was performed using LightCycler 480 SYBR Green I Master (Roche) and LightCycler 480 (Roche Diagnostics). The sequences of the oligonucleotides were as follows. 5'-GACCAACAAGTGTCTCCTCCAAA-3' (IFNβ; sense primer) and 5'-AGCAAGTTGTAGCTCATGGAAAGAG-3' (IFNβ; antisense primer); 5'-ATGTAGCCGCCCCACACAGACA-3' (IL-6; sense primer) and 5'-GCCAGTGCCTCTTTGCTGCTTTCA-3' (IL-6; antisense primer); 5'-AGGTGCAGTTTTGCCAAGGA-3' (IL-8; sense primer) and 5'-TTTCTGTGTTGGCGCAGTGT-3' (IL-8; antisense primer); 5'-ACTTTGGAGTGATCGGCCCCCAGA-3' (TNFα; sense primer) and 5'-GCTTGTCACTCGGGGTTCGAGAAGA-3' (TNFα; antisense primer); 5'-GCCAAGGTCATCCATGACAACT-3' (GAPDH; sense primer) and 5'-GAGGGGCCATCCACAGTCTT-3' (GAPDH; antisense primer). Target gene expression was normalized on the basis of GAPDH content.

References

1. R. Medzhitov, *Nature* **449**, 819 (2007).
2. K. Schroder, J. Tschopp, *Cell* **140**, 821 (2010).
3. O. Takeuchi, S. Akira, *Cell* **140**, 805 (2010).
4. M. Yoneyama, T. Fujita, *Immunol Rev* **227**, 54 (2009).
5. T. Tsuchida *et al.*, *Immunity* **33**, 765 (2010).
6. S. R. Paludan, A. G. Bowie, *Immunity* **38**, 870 (2013).
7. A. M. Krieg *et al.*, *Nature* **374**, 546 (1995).
8. H. Hemmi *et al.*, *Nature* **408**, 740 (2000).
9. H. Ishikawa, G. N. Barber, *Nature* **455**, 674 (2008).
10. B. Zhong *et al.*, *Immunity* **29**, 538 (2008).
11. W. Sun *et al.*, *Proc Natl Acad Sci U S A* **106**, 8653 (2009).
12. L. Jin *et al.*, *Mol Cell Biol* **28**, 5014 (2008).
13. H. Ishikawa, Z. Ma, G. N. Barber, *Nature* **461**, 788 (2009).
14. T. Abe *et al.*, *Mol Cell* **50**, 5 (2013).
15. H. Konno, K. Konno, G. N. Barber, *Cell* **155**, 688 (2013).
16. J. Wu *et al.*, *Science* **339**, 826 (2013).
17. L. Sun, J. Wu, F. Du, X. Chen, Z. J. Chen, *Science* **339**, 786 (2013).
18. A. Ablasser *et al.*, *Nature* **498**, 380 (2013).
19. D. L. Burdette *et al.*, *Nature* (2011).
20. Y. Tanaka, Z. J. Chen, *Sci Signal* **5**, ra20 (2012).

21. T. Abe, G. N. Barber, *J Virol* **88**, 5328 (2014).

22. T. Saitoh *et al.*, *Proc Natl Acad Sci U S A* **106**, 20842 (2009).

23. S. Ouyang *et al.*, *Immunity* **36**, 1073 (2012).

24. Q. Yin *et al.*, *Mol Cell* **46**, 735 (2012).

25. R. Misaki, T. Nakagawa, M. Fukuda, N. Taniguchi, T. Taguchi, *Biochem Biophys Res Commun* **360**, 580 (2007).

26. Y. Misumi *et al.*, *J Biol Chem* **261**, 11398 (1986).

27. A. Takatsuki, G. Tamura, *Agricultural and Biological Chemistry (Japan)* (1985).

28. G. Griffiths, S. Pfeiffer, K. Simons, K. Matlin, *J Cell Biol* **101**, 949 (1985).

29. D. Soulat *et al.*, *EMBO J* **27**, 2135 (2008).

30. M. J. De Brabander, R. M. Van de Veire, F. E. Aerts, M. Borgers, P. A. Janssen, *Cancer Res* **36**, 905 (1976).

31. S. Y. Dejgaard, A. Murshid, K. M. Dee, J. F. Presley, *J Histochem Cytochem* **55**, 709 (2007).

32. B. Zhong *et al.*, *Immunity* **30**, 397 (2009).

33. J. Zhang, M. M. Hu, Y. Y. Wang, H. B. Shu, *J Biol Chem* **287**, 28646 (2012).

34. Q. Wang *et al.*, *Immunity* **41**, 919 (2014).

35. Y. Qin *et al.*, *PLoS Pathog* **10**, e1004358 (2014).

36. C. Salaun, J. Greaves, L. H. Chamberlain, *J Cell Biol* **191**, 1229 (2010).

37. C. Aicart-Ramos, R. A. Valero, I. Rodriguez-Crespo, *Biochim Biophys Acta* **1808**, 2981 (2011).

38. K. Simons, M. J. Gerl, *Nat Rev Mol Cell Biol* **11**, 688 (2010).

39. A. Longatti *et al.*, *J Cell Biol* **197**, 659 (2012).

40. Y. Liu *et al.*, *N Engl J Med* **371**, 507 (2014).

41. N. Jeremiah *et al.*, *J Clin Invest* **124**, 5516 (2014).

42. S.-R. Woo *et al.*, *Immunity* **41**, 830 (2014).

43. L. Deng *et al.*, *Immunity* **41**, 843 (2014).

44. A. Rongvaux *et al.*, *Cell* **159**, 1563 (2014).

45. M. J. White *et al.*, *Cell* **159**, 1549 (2014).

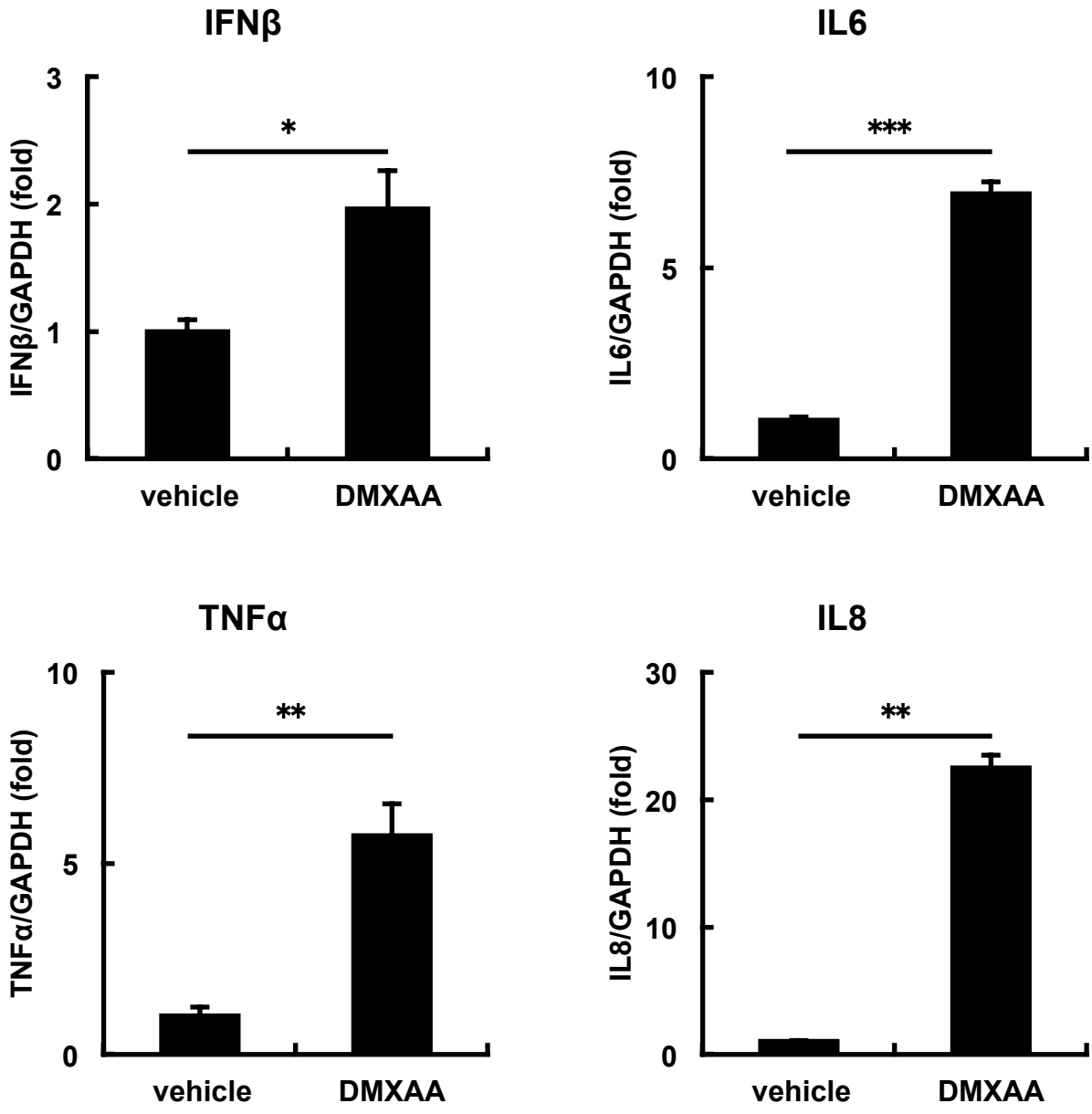

Fig. 1. DMXAA activates IRF3- and NF-κB- signaling pathways in emsCOS-1 cells that stably express EGFP-mouse STING (emsCOS-1)

The levels of mRNA of IFNβ, TNF-α, IL-6, and IL-8 were measured by quantitative RT-PC after 8 or 12 hours after the simulation of emsCOS-1 cells with DMXAA. The expression level of each gene is normalized to GAPDH gene and is represented as -fold induction over vehicle control. The data represent the mean ± SEM of n = 3 independent experiments, and were analyzed with one-way analysis of variance (ANOVA) followed by Tukey-Kramer post-hoc test. *$P < 0.05$; **$P<0.01$; ***$P<0.001$.

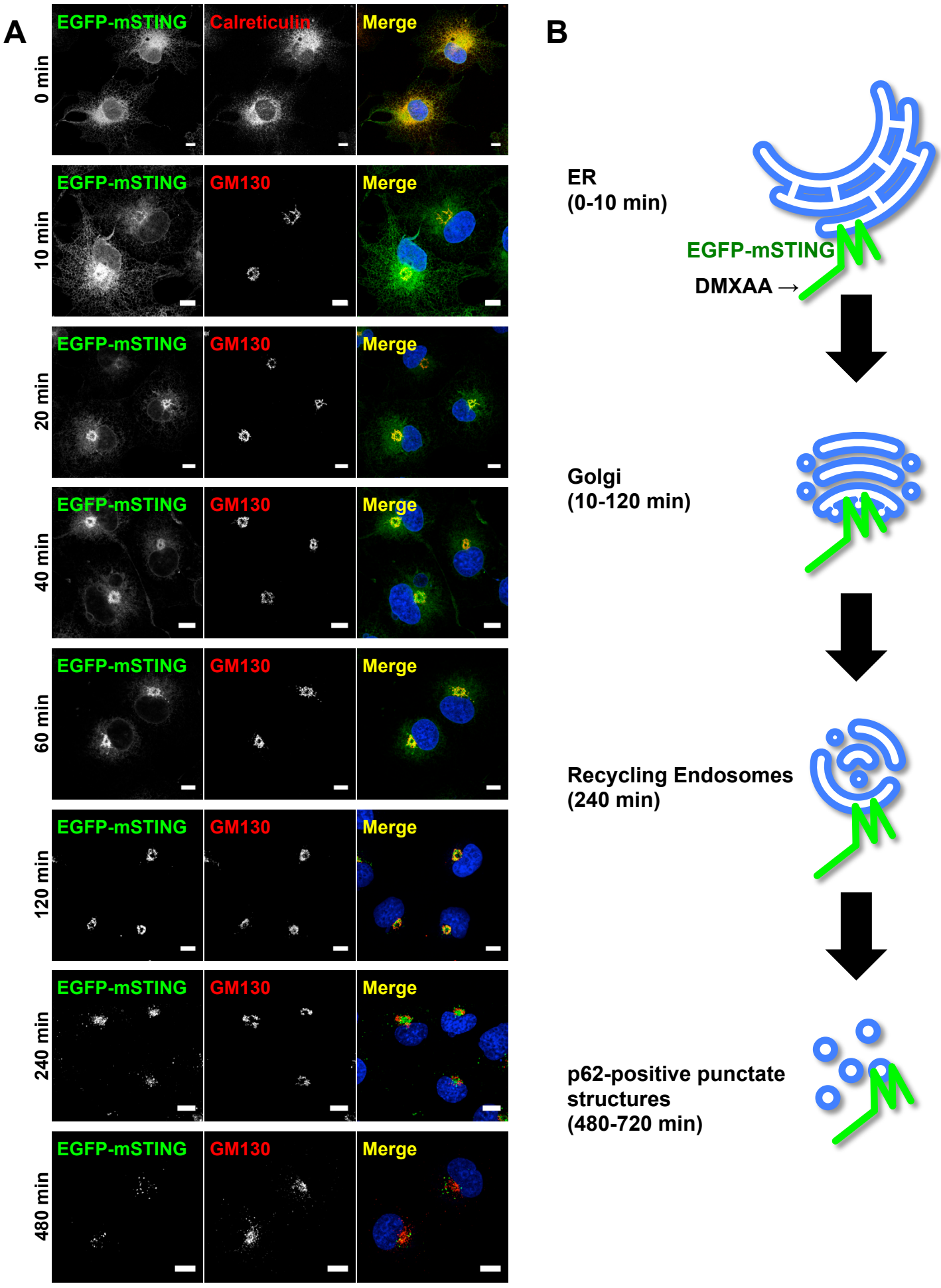

Fig. 2. Translocation of STING from the ER after DMXAA stimulation
(A) emsCOS-1 cells were stimulated with DMXAA (25 μg/mL), fixed, and stained for calreticulin (ER) or GM130 (Golgi). (B) An illustration to show the translocation of STING after its stimulation. Scale bar, 10 μm.

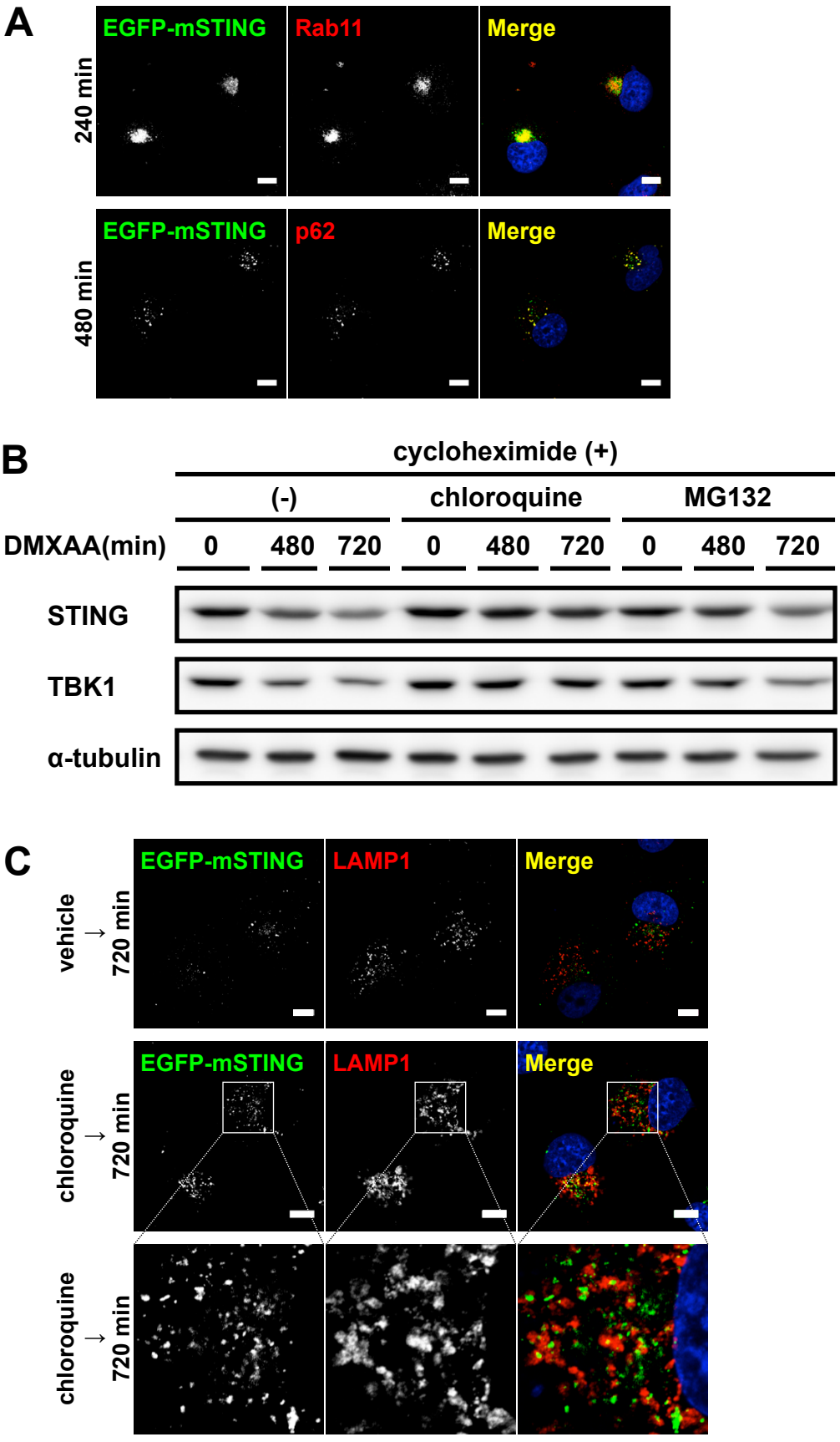

Fig. 3. STING was degraded in lysosomes 720 min after DMXAA stimulation.

(A) emsCOS-1 cells were stimulated with DMXAA (25 μg/mL), fixed, and stained for Rab11 (REs) or p62. Scale bar, 10 μm.

(B) emsCOS-1 cells were treated with chloroquine (100 μM) or MG132 (10 μM). At the indicated time after the stimulation with DMXAA (25 μg/mL), cell lysates were prepared and analyzed by WB. α-tubulin was used as a loading control.

(C) emsCOS-1 cells were treated with chloroquine (100 μM) and stimulated with DMXAA (25 μg/mL) for 720 min. Cells were then fixed and stained for LAMP1.

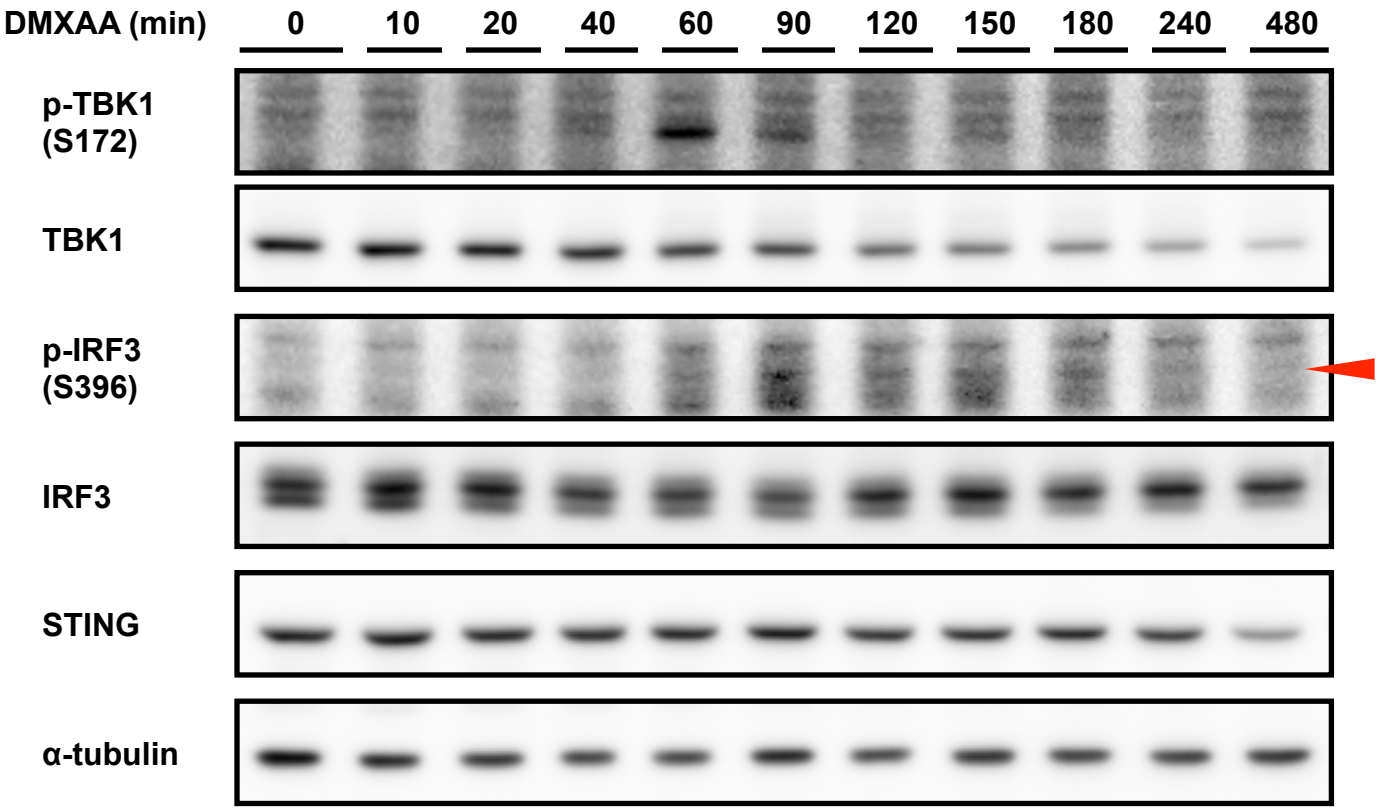

Fig. 4. DMXAA induced phosphorylation of TBK1 and IRF3 in emsCOS-1 cells
emsCOS-1 cells were stimulated with DMXAA (25 μg/mL) for the indicated time. Cell lysates were then prepared and analyzed by WB using antibodies against p-TBK1 (S172), TBK1, p-IRF3 (S396), IRF3, and STING. α-tubulin was used as a loading control. Red arrow head indicates p-IRF3 band.

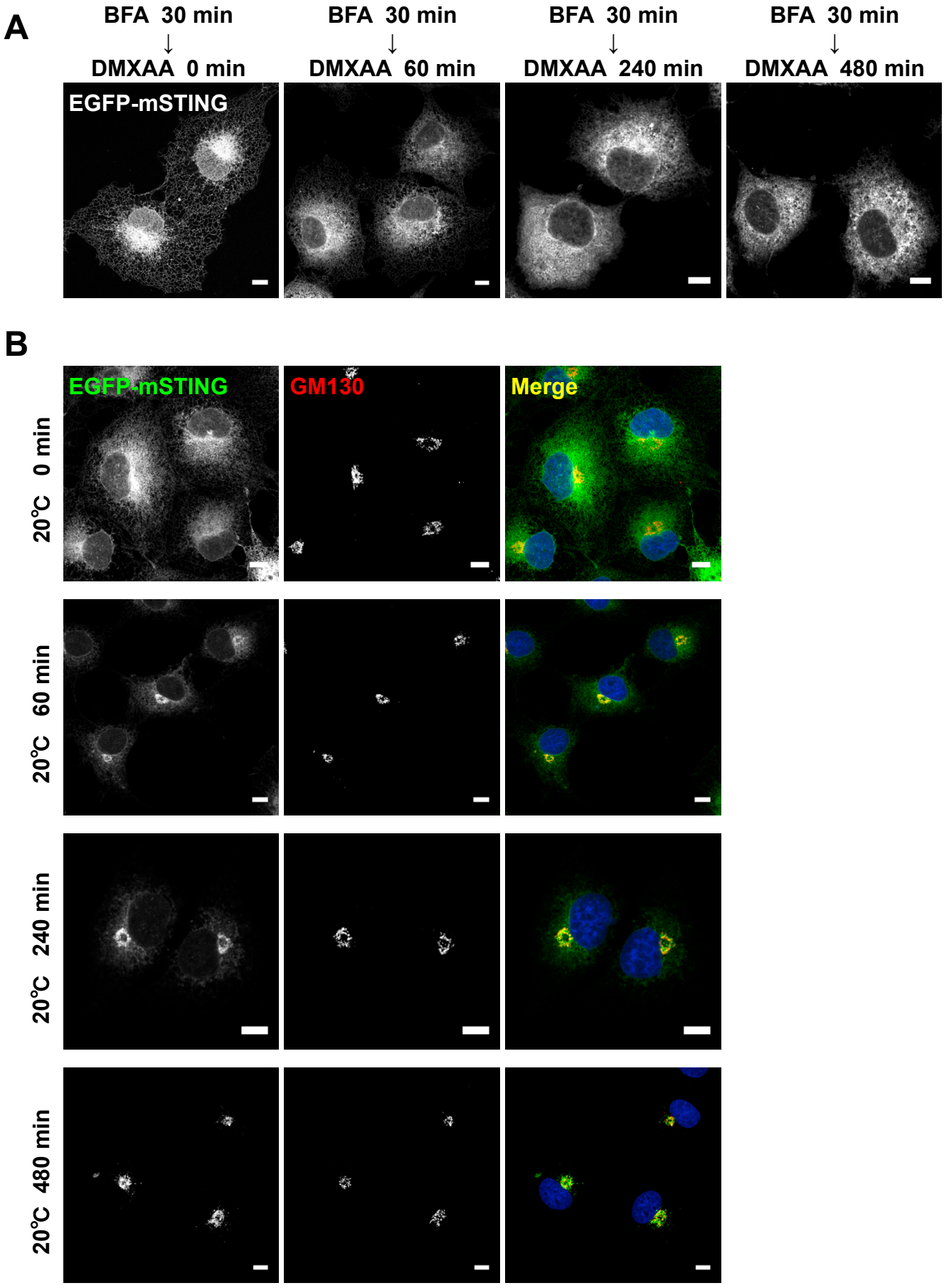

Fig. 5. The effect of BFA or 20°C treatment on the STING traffic

(A) emsCOS-1 cells were treated with brefeldin A (0.3 μg/mL) for 30 min. Cells were then stimulated with DMXAA (25 μg/mL) for the indicated time and fixed. Scale bar, 10 μm.

(B) emsCOS-1 cells were precultured at 20°C for 30 min. Cells were then stimulated with DMXAA (25 μg/mL) for the indicated time, fixed, and stained for GM130 (Golgi). Scale bar, 10 μm.

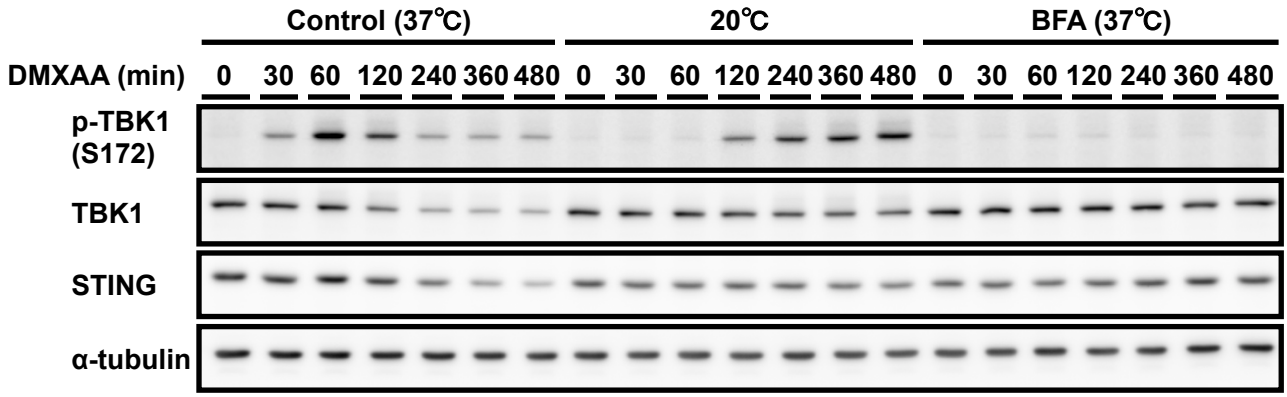

Fig. 6. The effect of the block of intracellular traffic of STING on TBK1 activation
To block the traffic from the ER, emsCOS-1 cells were treated with brefeldin A (0.3 μg/mL) for 30 min before DMXAA stimulation (25 μg/mL). To block the traffic from the Golgi, cells were precultured at 20°C for 30 min before DMXAA stimulation (25 μg/mL). Cell lysates were then prepared and subjected to WB using antibodies against p-TBK1 (S172), TBK1, and STING. α-tubulin was used as a loading control.

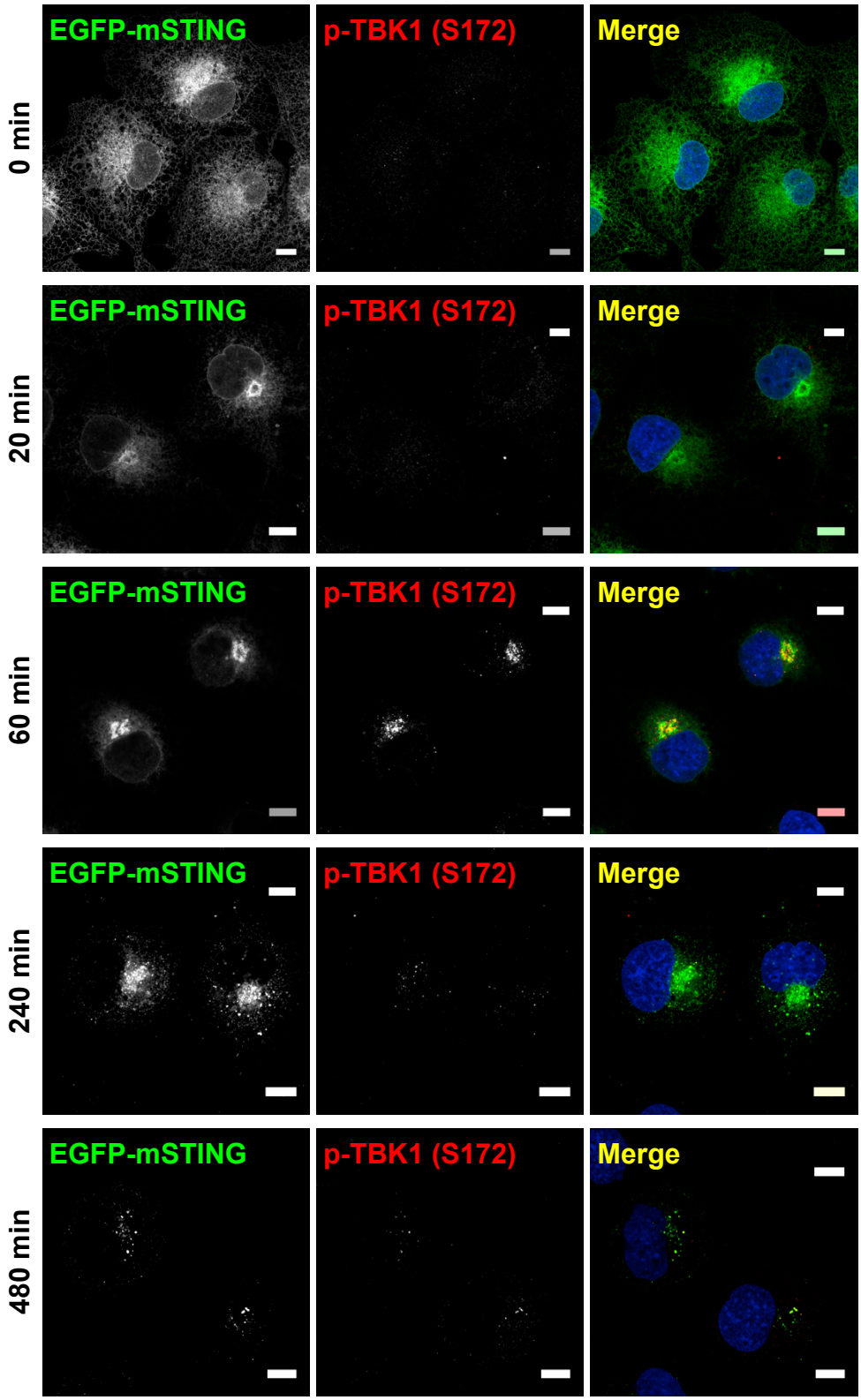

Fig. 7. Subcellular localization of p-TBK1 after DMXAA stimulation
emsCOS-1 cells were stimulated with DMXAA (25 μg/mL) for the indicated time, fixed, and stained for p-TBK1 (S172). Scale bar, 10 μm.

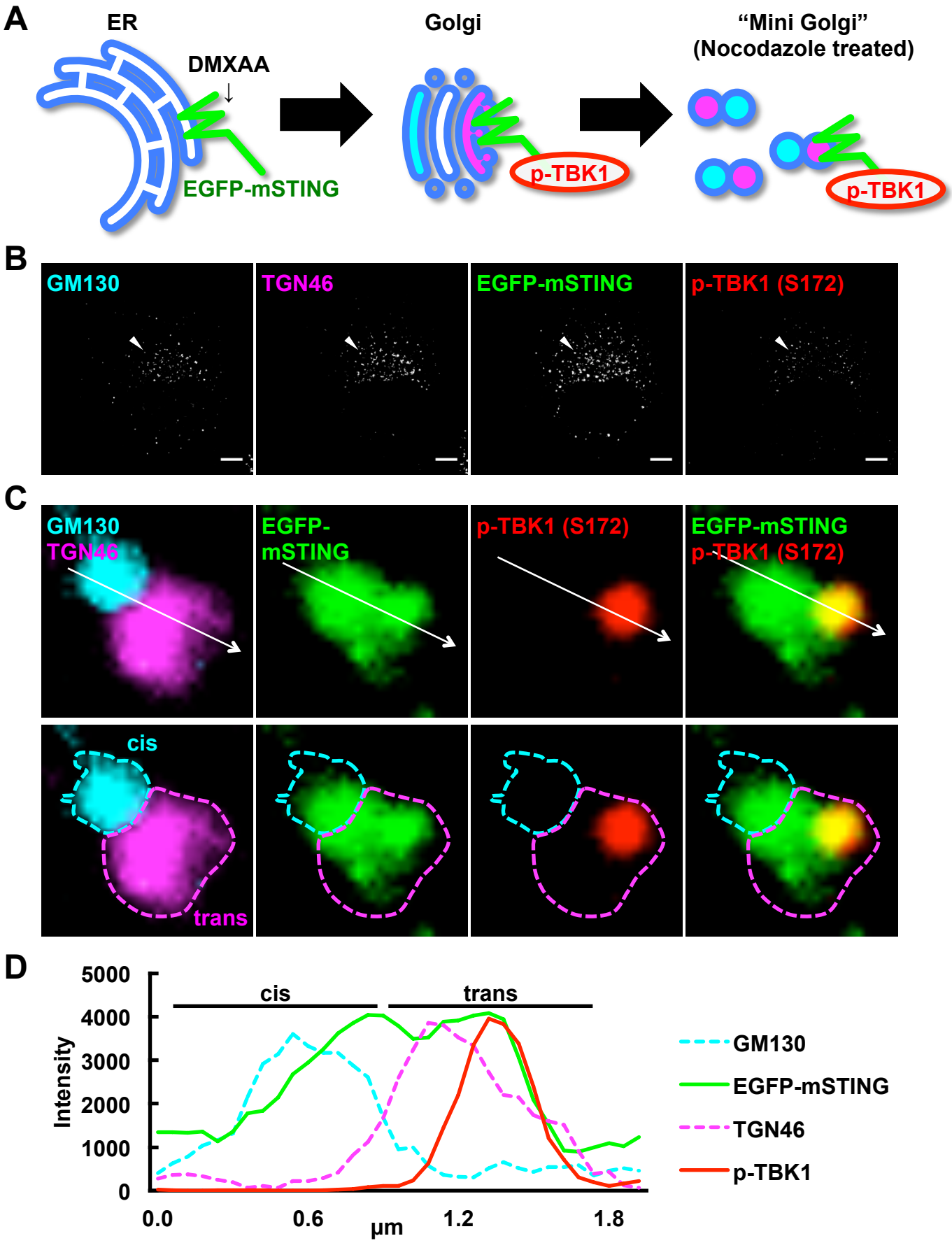

Fig. 8. TBK1 is activated at the trans-Golgi network (TGN)

(A) A model outlines the "Mini-Golgi" in the nocodazole- and DMXAA- treated emsCOS-1 cells.

(B) Cells were treated with nocodazole (6 μg/mL) for 30 min, then stimulated with DMXAA (25 μg/mL). Cells were fixed and stained for GM130 (cis-Golgi; cyan), TGN46 (TGN; magenta), p-TBK1 (red), and EGFP-mSTING (green). Scale bar, 10 μm.

(C) The magnified image of "Mini-Golgi" indicated by arrowheads in (B).

(D) Fluorescence intensity profile along the white arrow in (C).

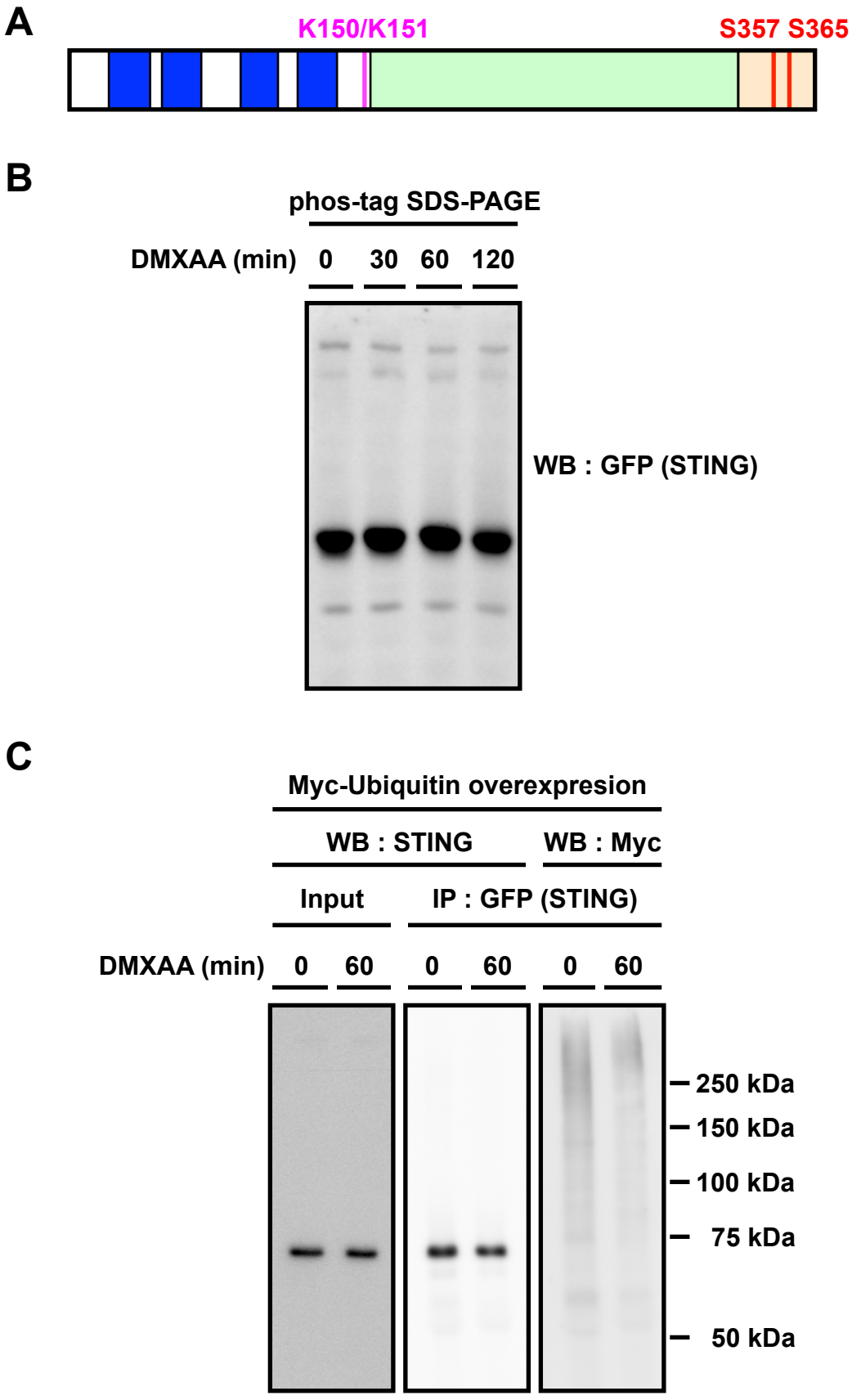

Fig. 9. STING is NOT phosphorylated or ubiquitinated in DMXAA-stimulated emsCOS-1 cells

(A) Schematic of STING indicating ubiqutination site (K150/K151; magenta), phosphorylation site (S357, S365; red), transmembrane domain (blue), and cyclic dinucleotides-binding domain (light green).

(B) After emsCOS-1 cells were stimulated with DMXAA (25 μg/mL) for the indicated time, cell lysates were prepared and subjected to phos-tag WB analysis using anti-GFP antibody.

(C) emsCOS-1 cells were transfected with myc-ubiquitine. Twenty-four hours after transfection, cells were stimulated with DMXAA (25 μg/mL). Cell lysates were immunoprecipitated with an anti-GFP antibody and immunoblotted with the indicated antibodies.

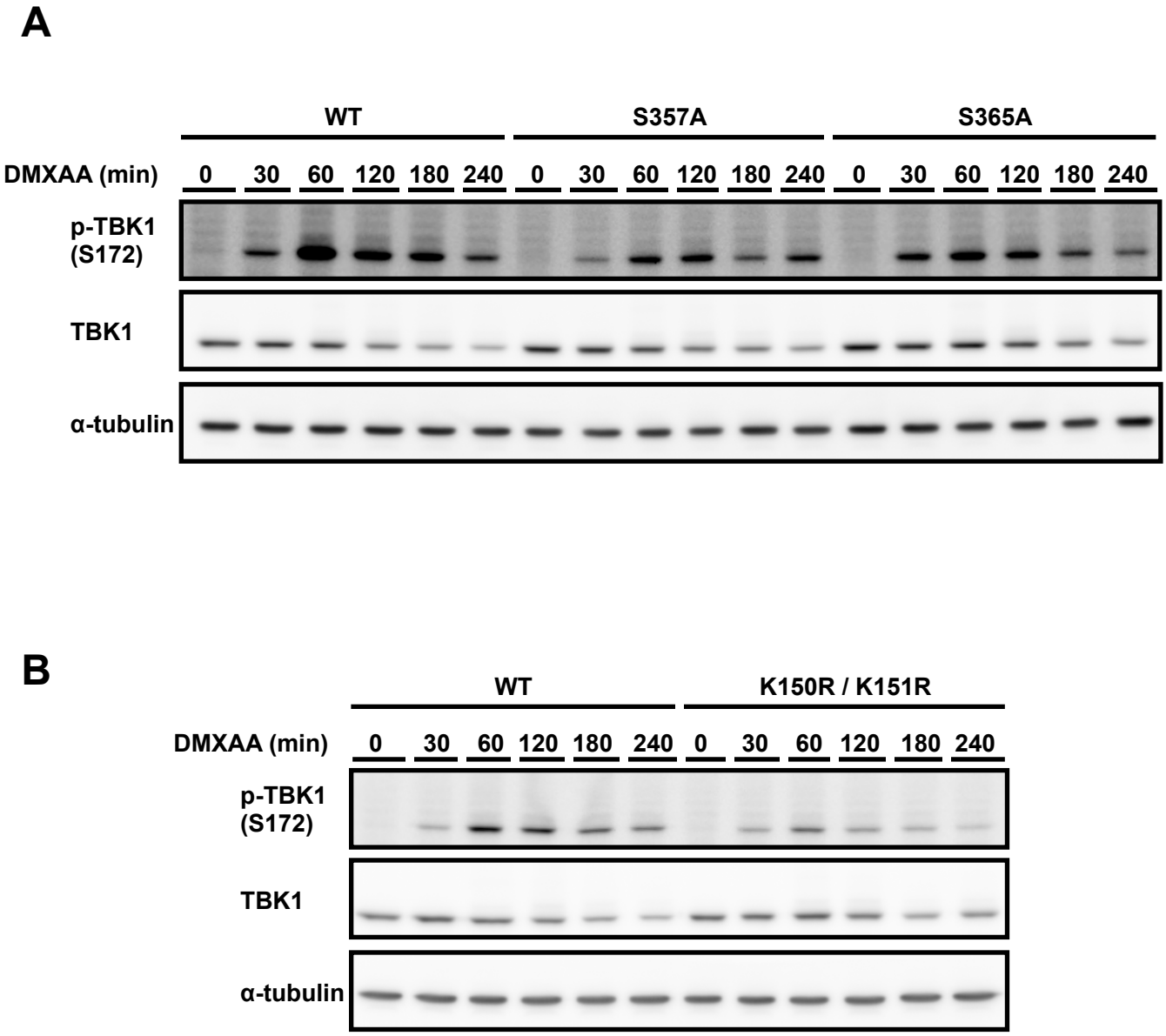

Fig. 10. Phosphorylation of S357, S365, or ubiquitination of K150/K151 on STING is NOT required for activation of TBK1

COS-1 cells that stably express STING with the indicated mutation were stimulated with DMXAA (25 μg/mL) and subjected to WB analysis using antibodies against p-TBK1 and TBK1. α-tubulin was used as a loading control.

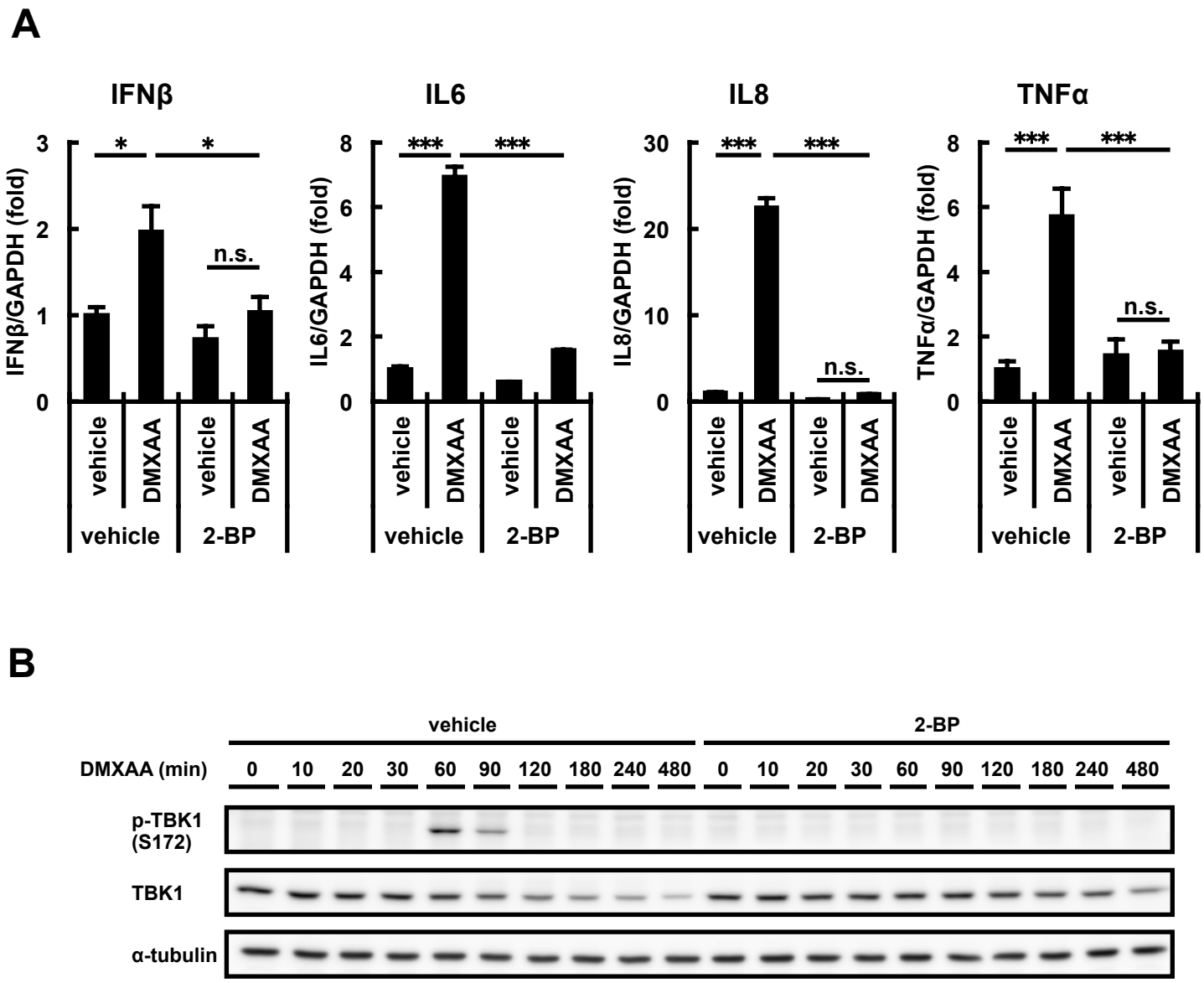

Fig. 11. 2-BP suppresses the activation of STING signaling pathway
emsCOS-1 cells were treated with 2-BP (50 μM) for 60 min, stimulated with DMXAA (25 μg/mL), and subjected to qPCR analysis (A) or WB analysis (B). The data represent the mean ± SEM of n = 3 independent experiments, and were analyzed with one-way analysis of variance (ANOVA) followed by Tukey-Kramer post-hoc test. **P* < 0.05; ***P*<0.01; ****P*<0.001; n.s., not significant.

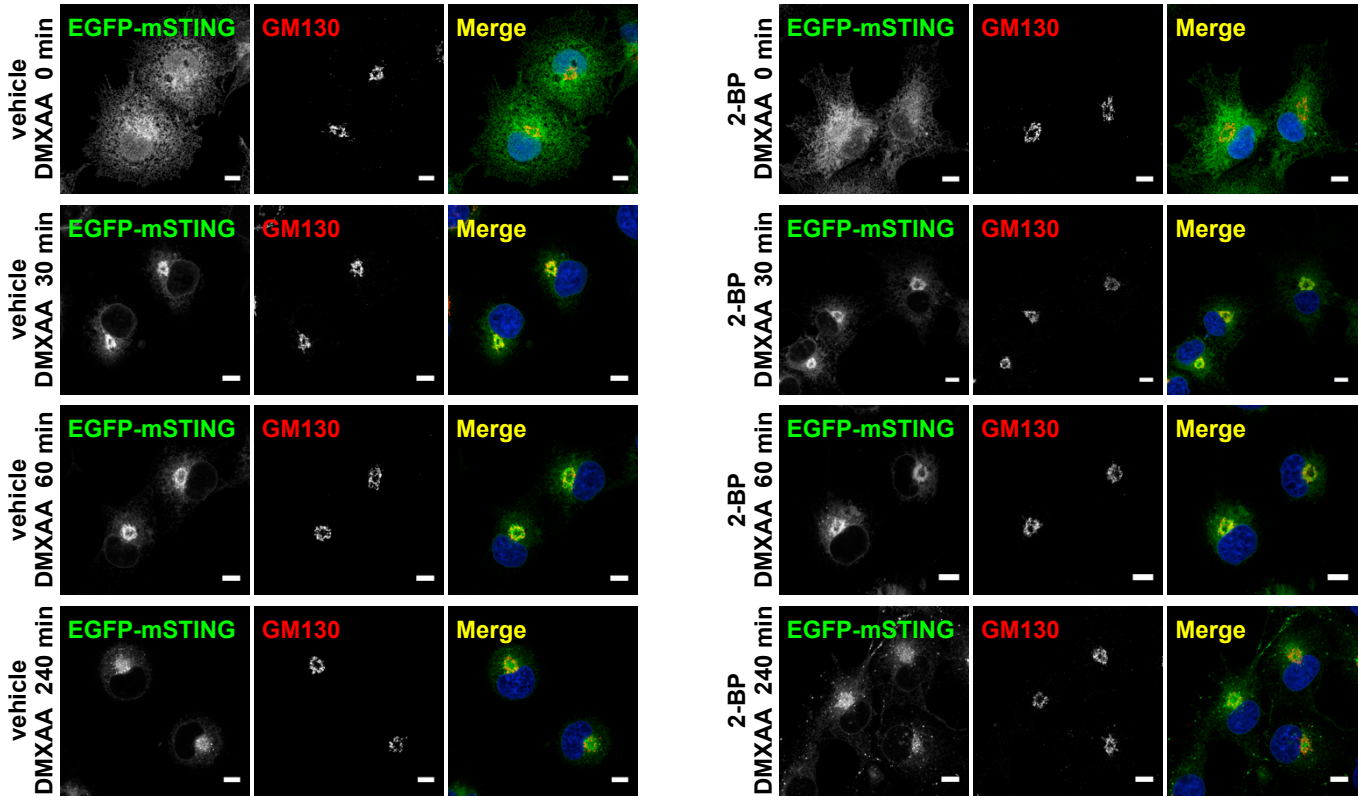

Fig. 12. 2-BP does NOT impair the translocation of STING from the ER
emsCOS-1 cells were treated with 2-BP (50 μM) for 60 min, stimulated with DMXAA (25 μg/mL), fixed, and staind for GM130. Scale bar, 10 μm.

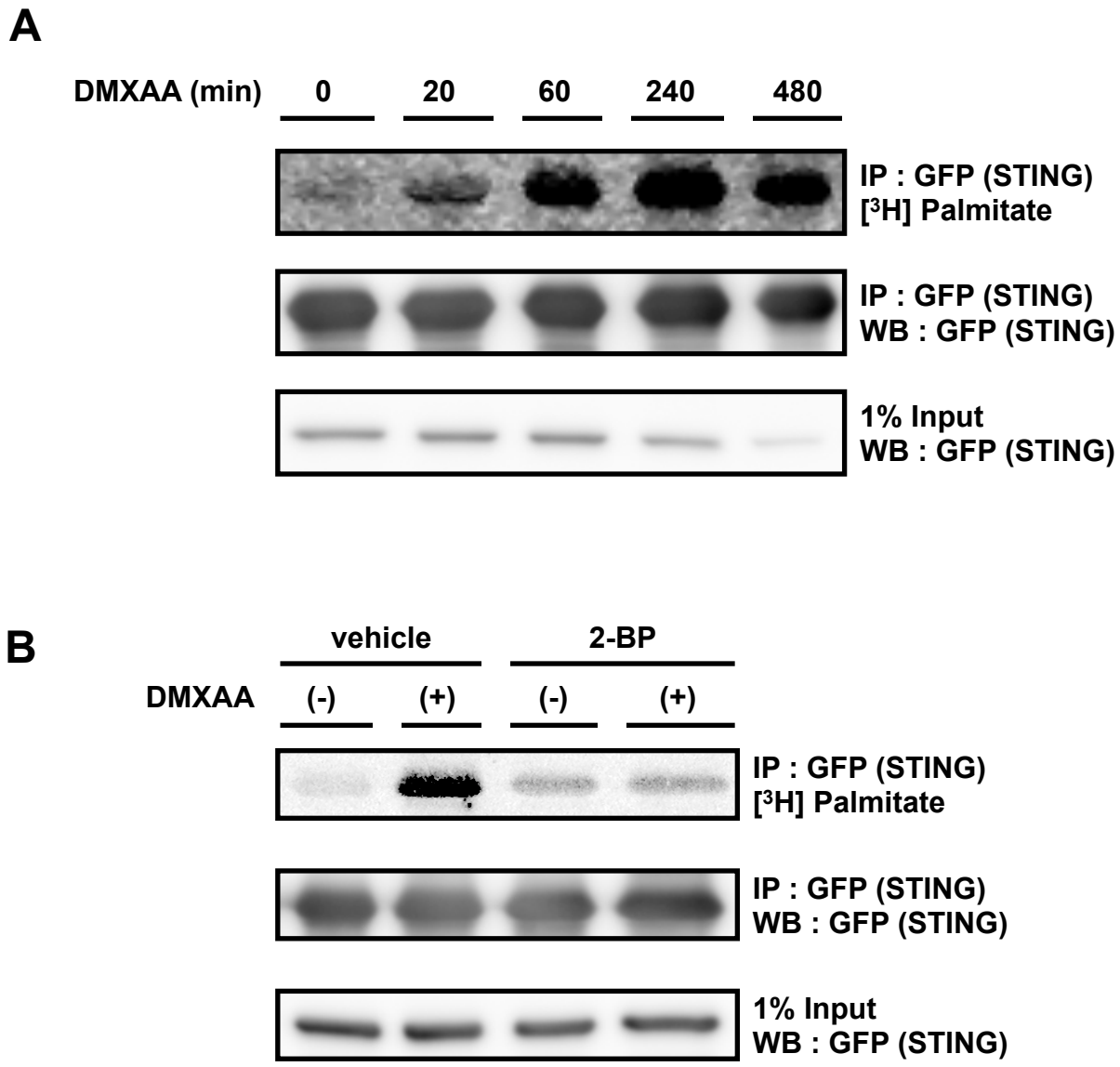

Fig. 13. DMXAA-dependent palmitoylation of STING

(A) emsCOS-1 cells were starved for 60 min, incubated with [^{3}H] palmitate for 60 min, and then stimulated with DMXAA (25 μg/mL) for the indicated time. STING was immunoprecipitated with anti-GFP antibody from the cell lysate, subjected to SDS-PAGE, and transferred to PVDF membrane. The radioactivity was detected by autradiograph. The amount of GFP-STING in immunoprecipipates was verified by WB (middle panel).

(B) Cells were starved for 60 min and incubated with 2-BP (50 μM) for 60 min. Cells were then incubated with [^{3}H] palmitate for 60 min and stimulated with DMSO or DMXAA (25 μg/mL) for 60 min. Cell lysates were subjected to the same procedure as in (A).

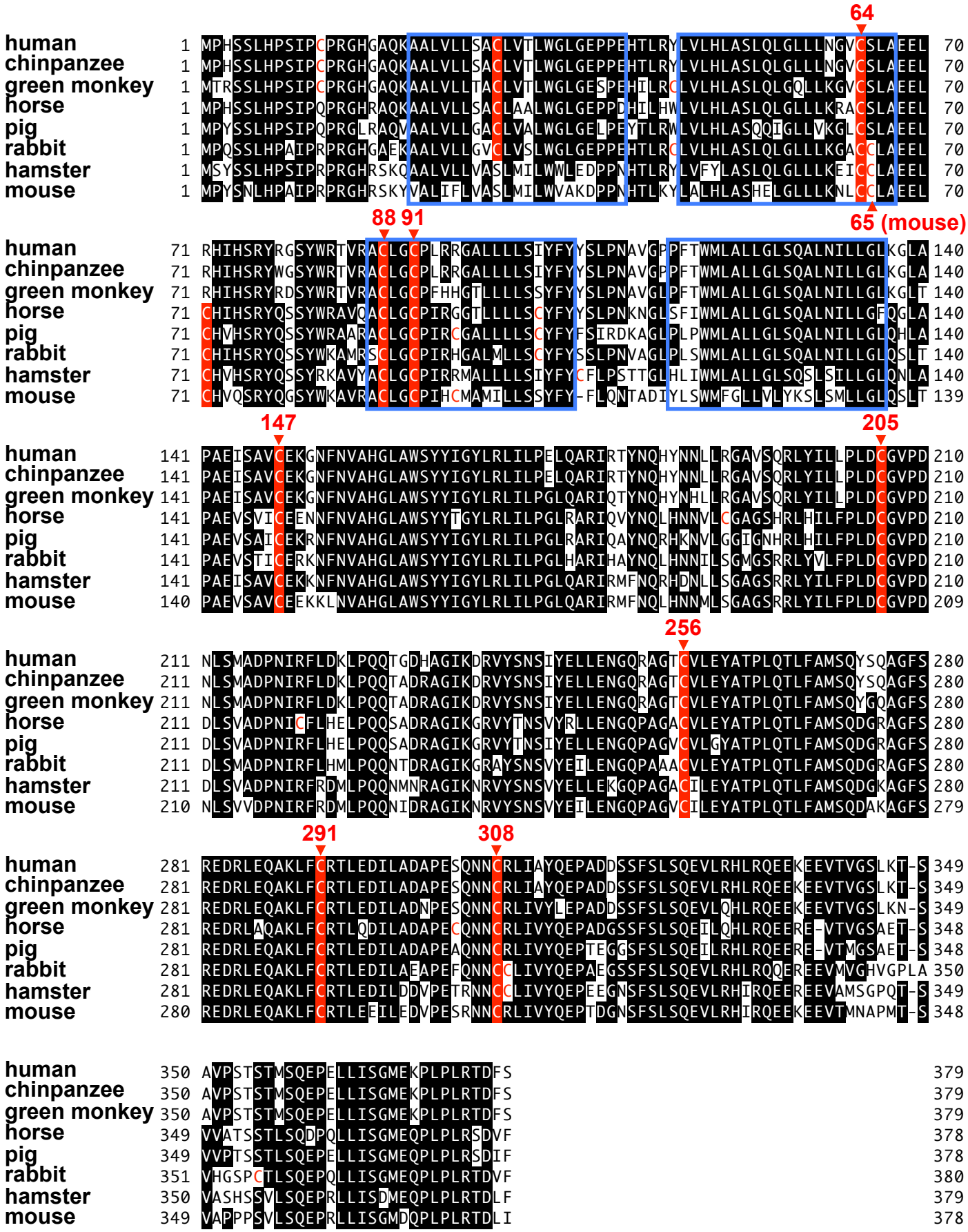

Fig. 14. STING has eight conserved cysteine residues in mammals
Comparison of the amino acid sequence of mammalian STING proteins. Red letters indicate cysteine residues and blue boxies indicate transmenbrane region (ref. uniprot).

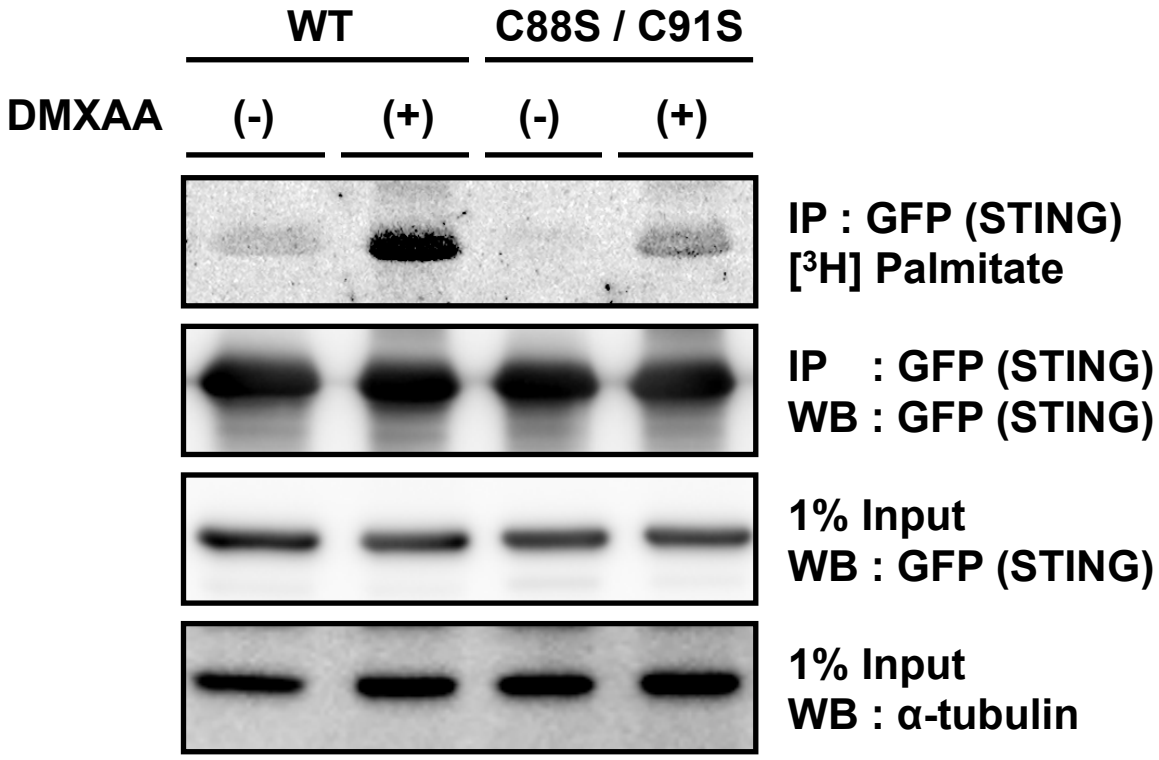

Fig. 15. C88 and/or C91 of STING is the primary site of palmitoylation(s).
COS-1 cells that stably express EGFP-mSTING (WT or C88S/C91S) were starved for 60 min, incubated with [^{3}H] palmitate for 60 min, and stimulated with DMXAA (25 μg/mL) for 60 min. Cell lysates were then prepared and subjected to the same procedure as in Fig. 13.

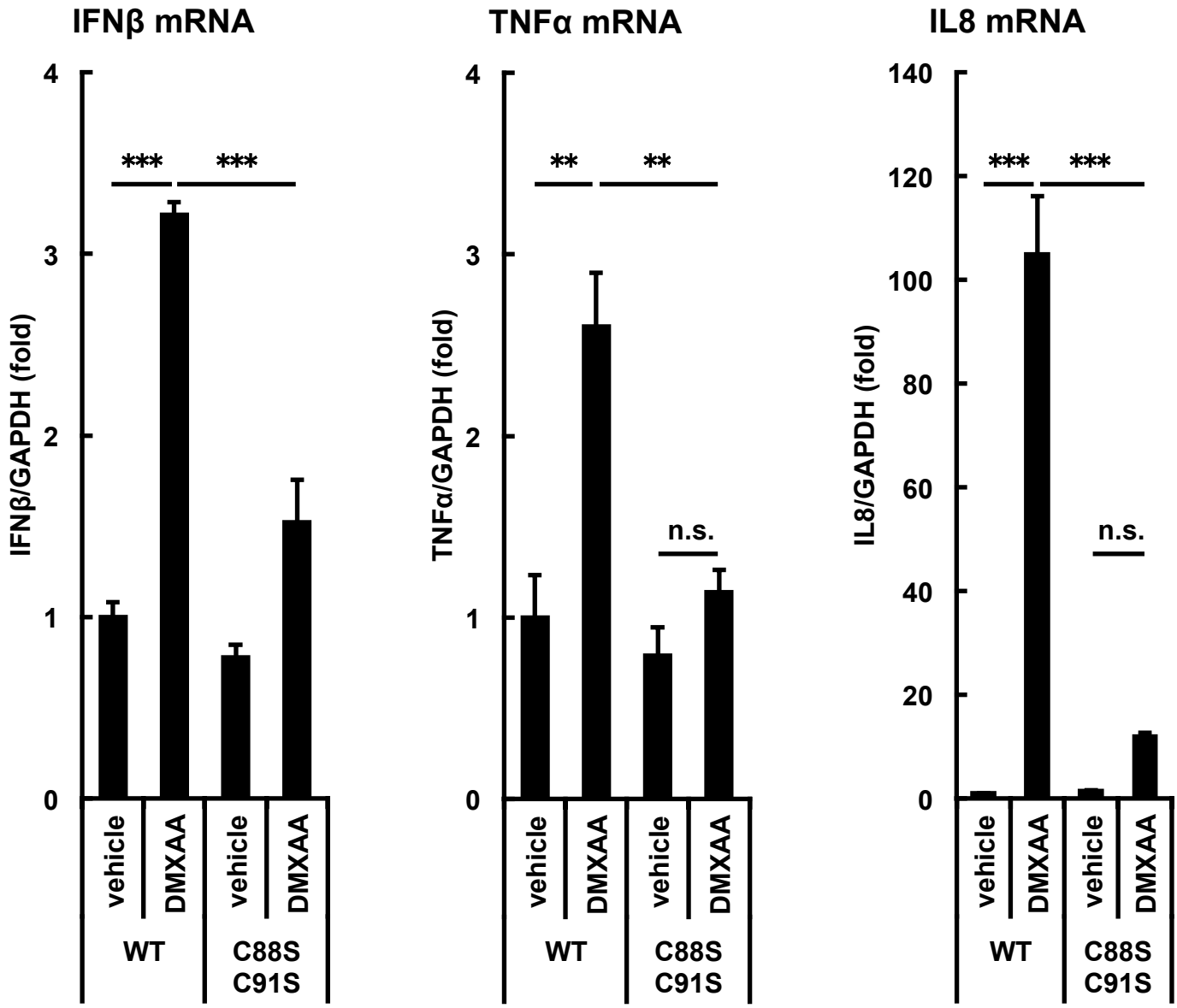

Fig. 16. Palmitoylation of C88 and/or C91 is required for STING signaling pathway
COS-1 cells expressing EGFP-mSTING (WT or C88S/C91S) were stimulated with DMXAA (25 μg/mL) for 8 hr. Cell lysates were then subjected to the qPCR analysis. The data represent the mean ± SEM of n = 3 independent experiments, and were analyzed with one-way analysis of variance (ANOVA) followed by Tukey-Kramer post-hoc test. *$P < 0.05$; **$P<0.01$; ***$P<0.001$; n.s., not significant.

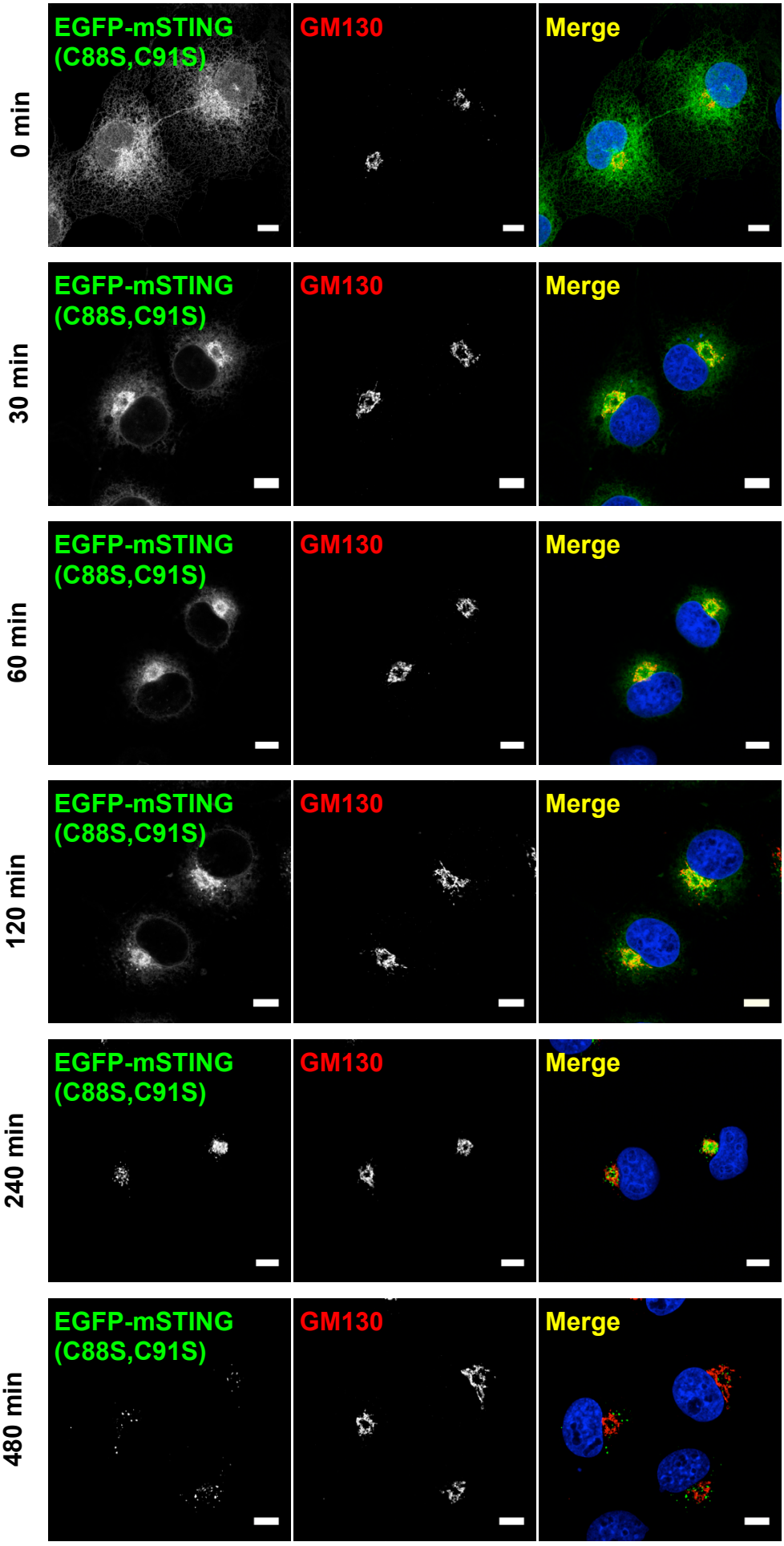

Fig. 17. Palmitoylation of C88 and/or C91 is NOT required for the traffic of STING
COS-1 cells expressing EGFP-mSTING (C88S/C91S) were stimulated with DMXAA (25 μg/mL), fixed, and stained for GM130. Scale bar, 10 μm.

Acknowledgements

本研究を進めるにあたり、終始御指導いただいた東京大学薬学部衛生化学教室の 新井洋由 教授、田口友彦 准教授、河野望 講師、今江理恵子 助教に心より感謝致します。また、大学院リサーチアソシエイトとして研究室に所属させていただき指導していただいた理化学研究所の小林俊秀 博士、および小林脂質生物学研究室の研究員の方々に感謝いたします。直接御指導下さいました田口友彦 准教授には本当にお世話になりました。この場を借りて暖かいご指導、ご鞭撻ご支援に深く感謝致します。

これまでの研究生活を共にし、本研究を様々な面で支えて下さいました衛生化学教室の皆さんに心より感謝致します。特に、これまで修士／博士課程でお世話になった河野望 講師、田中陸人 博士、有山博之 博士、嶋中雄太 修士、山守なつみ 修士、北井祐人 修士に深く感謝いたします。また、同じグループの李尚憲 修士、松平竜之 修士、寺坂慎平 学士、秋葉達也 君、仁木隆裕 学士、菅原小莉 さん、橋本啓志 君に心より感謝致します。また、同期として苦楽をともにした、大場陽介 修士には大変感謝しています。努力を惜しまない優秀な同期に囲まれ、自分も妥協なく研究に勤しむことができました。実験のサポートをしていただいた福田英子さん、高田祥恵さんに心より感謝します。

いつも応援し、暖かく見守ってくれた父、母、兄、祖母、叔父に心より感謝します。最後に、同じくいつも暖かく見守ってくれた亡き祖母に心より感謝します。

本当にありがとうございました。　　２０１５年1月９日